



HAL
open science

A general theory of rock glacier creep based on in-situ and remote sensing observations

Alessandro Cicoira, Marco Marcer, Isabelle Gärtner-roer, Xavier Bodin, Lukas
Arenson, Andreas Vieli

► **To cite this version:**

Alessandro Cicoira, Marco Marcer, Isabelle Gärtner-roer, Xavier Bodin, Lukas Arenson, et al. A general theory of rock glacier creep based on in-situ and remote sensing observations. *Permafrost and Periglacial Processes*, 2020, 10.1002/ppp.2090 . hal-03082968

HAL Id: hal-03082968

<https://hal.science/hal-03082968>

Submitted on 21 Dec 2020

HAL is a multi-disciplinary open access archive for the deposit and dissemination of scientific research documents, whether they are published or not. The documents may come from teaching and research institutions in France or abroad, or from public or private research centers.

L'archive ouverte pluridisciplinaire **HAL**, est destinée au dépôt et à la diffusion de documents scientifiques de niveau recherche, publiés ou non, émanant des établissements d'enseignement et de recherche français ou étrangers, des laboratoires publics ou privés.

RESEARCH ARTICLE

WILEY

A general theory of rock glacier creep based on in-situ and remote sensing observations

Alessandro Cicoira^{1,2}  | Marco Marcer³  | Isabelle Gärtner-Roer¹ |
Xavier Bodin³  | Lukas U. Arenson⁴  | Andreas Vieli¹ 

¹Department of Geography, University of Zurich, Switzerland

²Department of Geosciences, University of Fribourg, Switzerland

³Laboratoire EDYTEM, Centre National de la Recherche Scientifique, Université Savoie Mont Blanc, Le Bourget-du-Lac, France

⁴BGC Engineering Inc., Vancouver, BC, Canada

Correspondence

Alessandro Cicoira, Department of Geography, University of Zurich, Switzerland.
Email: alessandro.cicoira@geo.uzh.ch

Funding information

nano-tera.ch, Grant/Award Number: ref. no. 530659

Abstract

The ongoing acceleration in rock glacier velocities concurrent with increasing air temperatures, and the widespread onset of rock glacier destabilization have reinforced the interest in rock glacier dynamics and in its coupling to the climate system. Despite the increasing number of studies investigating this phenomenon, our knowledge of both the fundamental mechanisms controlling rock glacier dynamics, and their long-term behaviour at the regional scale remain limited. We present a general theory to investigate rock glacier dynamics, its spatial patterns and temporal trends at both regional and local scale. To this end, we combine a model to calculate rock glacier thickness with an empirical creep model for ice-rich debris, in order to derive the Bulk Creep Factor (BCF), which allows to disentangle the two contributions to the surface velocities from (i) material properties and (ii) geometry. Thereafter, we provide two examples of possible applications of this approach at a regional and local scale.

KEYWORDS

bulk creep factor BCF, destabilization, permafrost creep, regional scale, rock glacier dynamics, thickness model

1 | INTRODUCTION

Rock glaciers are creeping masses of frozen debris shaping the mountain periglacial environment. The very definition of rock glaciers has been inextricably intertwined with their dynamics since the first scientific publications on these landforms.¹ In fact, the surface appearance and the down-valley motion of rock glaciers are the visible expressions of their internal deformation, which depends on the internal stresses and on the physical properties of their constitutive material (Figure 1). For decades, rock glaciers were thought to creep down slope driven by gravity at a constant rate, in secondary creep stage and almost independent of any external influence.² Starting in the 1980s, kinematic observations have highlighted strong inter-annual and seasonal variability in rock glacier flow velocities, arousing renewed interest in their dynamics and in the processes that control it.³ Based on detailed kinematic data, statistical and numerical modelling

have been used to link the observed temporal fluctuations in creep velocities at different time scales to climatic forcing such as air and ground temperature, snow melt, and liquid precipitation.^{4–8} Further, the onset of rock glacier destabilization, i.e. the sudden and exceptional acceleration of (a part of) the deforming rock glacier, has been related to positive air temperature anomalies under appropriate topographical conditions.^{9,10}

Although our knowledge of surface kinematics of rock glaciers is very detailed^{11–15} only a limited number of studies have investigated their internal structure and physical properties.^{16–18} This paucity in direct observations is caused in the first place by the extreme effort needed to investigate the complex interior of a rock glacier and the periglacial environment in general.¹⁹ Rock glacier velocities are often directly or relatively compared (kinematic level), neglecting the influence of their material properties, geometry and stresses (dynamics level). Few more sophisticated physical and mathematical approaches

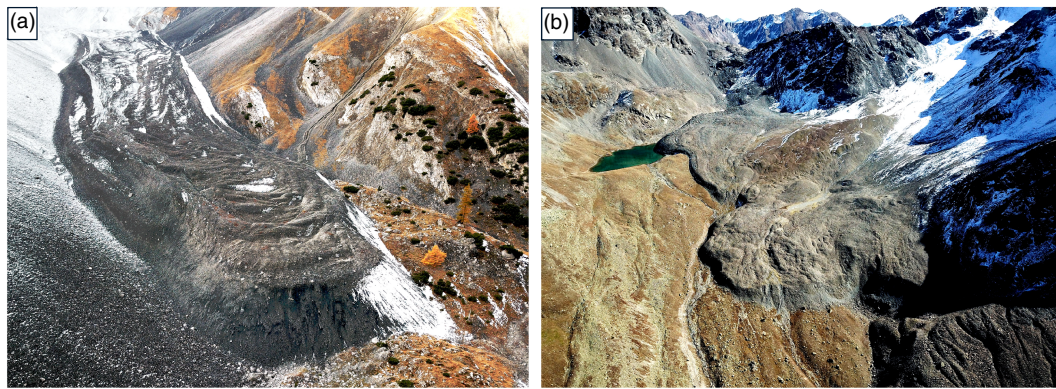


FIGURE 1 Rock glaciers can be simple landforms, manifesting essential geometries and flow patterns, or in the contrary they can exhibit very complex dynamics and morphology. In this figure, the Val dall'Acqua Rock Glacier located in the homonym valley (a) and the Gianda Viva rock glacier complex in the Muragl Valley (b) illustrate two extremes of this variety [Colour figure can be viewed at wileyonlinelibrary.com]

have so far been proposed to describe rock glacier dynamics,^{6,8,20–23} but they are hardly re-applied in other studies. Inevitably, the above limitations inhibit interdisciplinary studies and hamper the interpretation and analysis of the climatic, geomorphological and hydrological significance of rock glaciers at all temporal and spatial scales. In addition, such limitations lead to misinterpretations and confusion amongst the scientific community and the general public.

In this paper, we propose a general conceptual and physically based model in order to overcome the above mentioned limitations and facilitate spatio-temporal investigations of rock glacier creep. First, in Section 2, we summarize the current knowledge on the internal structure of rock glaciers and on the physical processes controlling their motion, based on in-situ investigations and laboratory experiments. This brief review is tailored to the information needed to develop our conceptual and mathematical model. For a more comprehensive summary of the deformation of debris-ice mixtures the readers are referred to the two thorough reviews from Arenson et al.²⁴ and Moore.²⁵ Section 3 is focused on the derivation and mathematical formulation of our general approach to investigate rock glacier creep. After a short review of the rheological models for rock glaciers, we analyse a comprehensive dataset of rock glacier thickness, slope and surface velocity. On this basis, we propose a mathematical formulation to describe rock glacier dynamics, which combines a perfectly plastic model to calculate rock glacier thickness with an empirical creep model for ice-rich debris (Section 3.3). The formulation leads to the definition of the Bulk Creep Factor (BCF), which represents the properties of the rock glacier material. The proposed methodology thereby allows to disentangle the geometrical and the rheological contributions to the velocity signal. It embodies a trade-off between complexity and oversimplification. After presenting a physical interpretation of the BCF, we briefly illustrate two real-world applications at regional and local scale. First, we analyse the dynamic behaviour of 414 rock glaciers from Austria, France, Italy, and Switzerland and explore the variability in the BCF. Second, we use detailed kinematic observations to investigate and compare the spatial variability in surface creep velocities of three rock glaciers which are characterised by contrasting dynamical behaviour: (slow) steady-state creep, abnormal

fast creep, and destabilization. Finally, we critically discuss the limitations and further potential applications of the proposed approach.

2 | A PHYSICAL DESCRIPTION OF ROCK GLACIER CREEP

In early studies, the movement of rock glaciers has been thought to happen mostly near the surface and being driven by freeze-thaw cycles.¹ Almost fifty years later, Wahrhaftig and Cox² deduced solely from geomorphological observations that a large part of the deformation within a rock glacier must occur at depth. Their hypothesis was confirmed only in recent years, when direct observations from borehole investigations shed light on the internal structure and deformation profile of rock glaciers.²⁶ Although only limited direct observations exist, the borehole data show a recurrent structure and behaviour for all the investigated landforms.^{16,18,27–29} Based on this knowledge, rock glaciers are typically divided into three distinct structural and dynamical units, which are, from the surface to deeper ground: the active layer, the ice-rich core, and the shear horizon. Below these three units no or very limited movement occurs: the shear horizon delimits in a dynamic sense the thickness of the active rock glacier itself. The surface displacements of a rock glacier are the sum of the three independent contributions described below. In the following sections, we present a brief review of our current knowledge on the physics of permafrost creep and rock glacier dynamics, essential for their mathematical description.

2.1 | The active layer

At the rock glacier surface, a few meters of seasonally frozen blocky sediments represent the interface between the ice-rich permafrost and the atmosphere. The thermodynamics of the active layer are complex due to the multiphase nature of this layer, which consists of a rock, ice, water, and air fraction, and because of the multitude of processes governing its energy balance, which include conductive,

advective, and convective heat fluxes.^{30–33} During the summer months, the active layer insulates the permafrost underneath it, preventing or strongly reducing the thawing process at the permafrost surface. Although melt rates at degrading rock glacier sites are usually limited to a few centimeters per year,²⁸ the influence of increasing air temperature can significantly (exponentially) impact the creep rates of the underlying rock glacier.^{5,6,34,35}

The deformation of the active layer is mostly linked to tilting or sliding of the boulders on top of the permafrost table. Rare events of active layer detachments have been observed at rock glacier sites, characterised by extreme rates of displacement due to sliding.^{36,37} In some cases, boulders can move very rapidly for a short time also in relation to tilting. In fact, when a boulder is tilting close to a terrain step, it might lose its stability and quickly roll down slope, as it often happens close to the active front.^{26,38} When measuring surface displacements, it is difficult to filter the deformation component associated to the active layer. Nevertheless, the magnitude of this component is in general orders of magnitude smaller than the total surface velocity, therefore negligible in first approximation.^{8,13} An exception might be slow-moving rock glaciers, where the movement of the boulders on the surface can represent a relevant contribution to the total observed velocities (e.g. Murtél Rock Glacier, unpublished data). Based on this evidence, the dynamics of the active layer can be neglected in the forthcoming mathematical description of rock glacier creep. However, it is important to remember that the active layer is essential for the surface mass and energy balance of a rock glacier and thereby has a strong influence (as we will see in the next section) on rock glacier dynamics.

2.2 | The ice-rich core

The inner core of a rock glacier is composed of a mixture of ice and debris with a typical thickness of 10 to 25 m. The ice component can be polygenetic and may include significant meteoric, superficial, and ground-water contributions.³⁹ Observations from boreholes at moving rock glaciers indicate values of the volumetric ice content of above 50% apart from the case of degrading permafrost conditions, where the values can be lower.^{5,16,40,41} The debris component of rock glaciers typically originates from debris-laden snow avalanches, episodic rock avalanches and long-lasting rockfall activities.^{40,42,43} The grain size of the debris component is usually finer than in the active layer. This structural difference is the consequence of the processes that contribute to the debris supply (fall sorting and washing away) and the motion of the rock glacier itself (kinetic sieving).⁴⁰ As a consequence, the structure of the ice-debris matrix can be very heterogeneous within a single rock glacier and can be very diverse amongst different landforms.^{42,44} The thermal regime of the inner core is mainly controlled by heat conduction. Therefore, the phase of the temperature signal from the surface is linearly delayed and its amplitude exponentially attenuated with depth.^{8,45} The seasonal temperature signal influences the frozen ground down to the depth of the zero amplitude, which is usually found at about 10 to 20 m depth. Thermal changes

below this depth require temperature forcing to act at longer temporal scales (decades and beyond). With regard to water flow, the ice-rich core can be considered impermeable in first approximation.⁴⁶ However, water flow has the potential to affect the inner core especially under conditions of permafrost degradation, when temperatures close to the melting point lead to high structural heterogeneity, preferential flow pathways and augmented interstitial water content (ibidem).

The deformation of the ice-rich core is mainly governed by the time dependent creep of its ice component.²⁴ Similarly to pure ice, the creep of the inner core is susceptible to temperature variations and depends on the structure of the rock glacier itself. More specifically, the creep behaviour of a debris-ice mixture and even its stress-strain behaviour (ductile - dilatant - brittle) can vary substantially depending on the applied strain rate, on the volumetric ice content and on the grain size of the debris component.²⁴ For a homogeneous matrix, the ice-rich core can be described as a creeping viscous material, as confirmed by the classical deformation profiles observed from inclinometer readings (see Figure 2). However, for more heterogeneous and anisotropic structures, the debris component and the ice structure can strongly influence the deformation profile.¹⁸ Overall, an amount of 10%-40% of the total displacement takes place within the ice-rich core and is governed by temperature variations.¹⁶

2.3 | The shear horizon

The shear horizon is a shallow layer of a few meters of thickness, where the highest shear rates are observed and where most of the deformation (60%-90%) occurs.¹⁶ It is located below the inner core, at a depth of 15 to 30 m from the surface. Despite the extreme paucity of observations, borehole investigations consistently showed a decrease in volumetric ice content (20%-50%) and in the debris grain size within this layer.^{27,34} Moreover, in the shear horizon, the large deformation rates may modify the structure and influence the properties of the material itself, as suggested by the banded ice observed in the ice cores from the Lazaun Rock Glacier in Sudtiroil (IT).²⁸ Due to the depth of the shear horizon, the influence of surface temperature forcing is limited and considerably delayed in time.^{4,7} At longer time scales, however, changes in temperature, especially in intervals close to the melting point can substantially affect the mechanical properties of the rock glacier material, also at depth of the shear horizon. While the ice-rich core can be assumed to be mostly impermeable to water flow, pressurised water has been observed during borehole perforations within the shear horizon, suggesting a strong influence from unfrozen water on the behaviour of this unit.^{17,18,47}

Debris-ice mixtures are usually more resistant to deformation at low temperatures than their pure end-member components.²⁵ As a consequence, the apparent viscosity of rock glacier material is larger than for pure ice at the same temperature and stress.^{5,6} However, especially close to melting conditions, the growth of unfrozen water films at the interface between ice and debris has the potential to reduce the strength of the mixture and can even lead to substantial weakening.²⁵ In accordance to this consideration, the effective

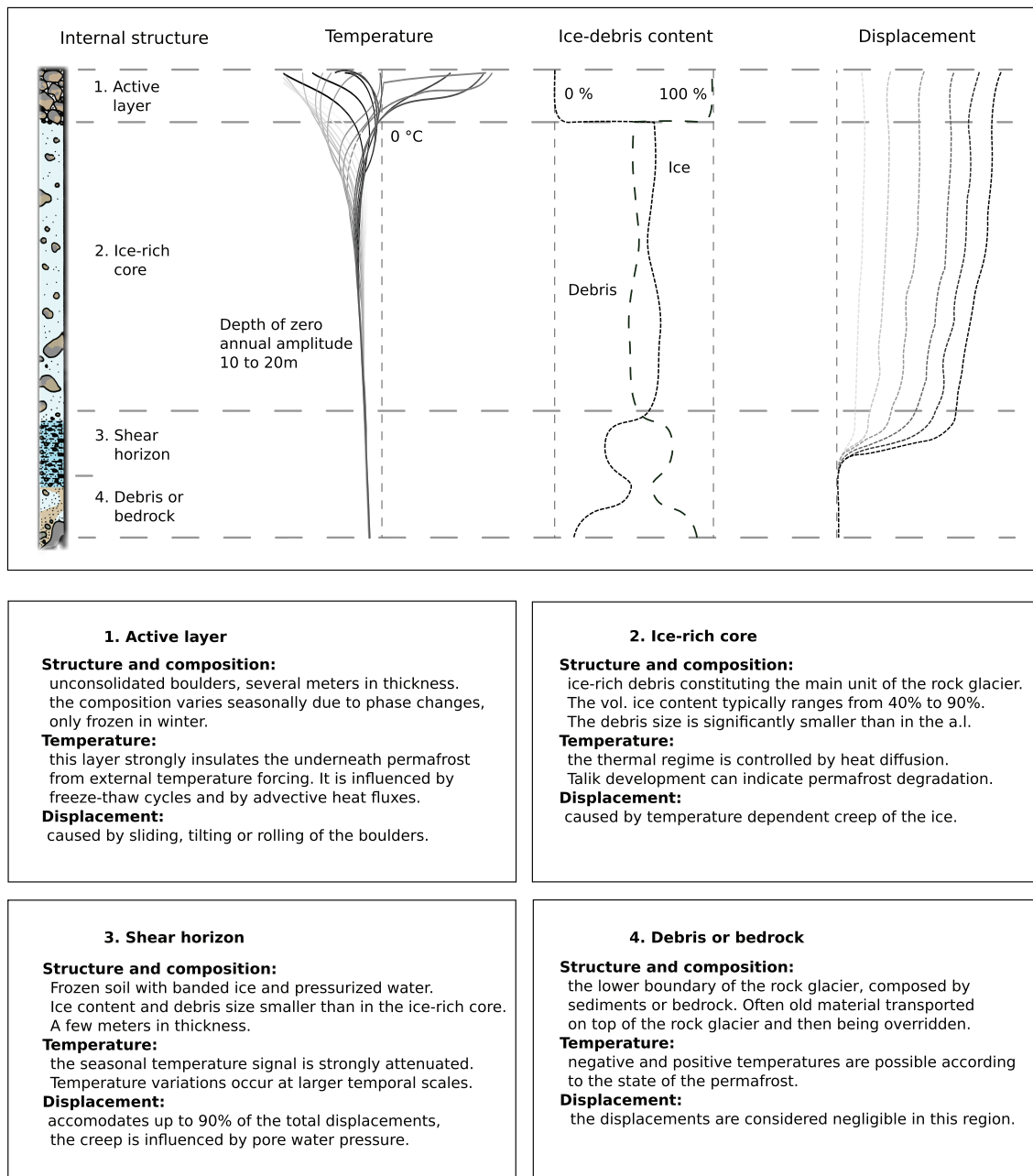


FIGURE 2 Graphical illustration and textual description of vertical profiles (conceptualised) of a typical rock glacier. From left to right the internal structure, the ground temperature variations, the material composition and the displacement profiles of a typical rock glacier are shown. The concept is based on the most influencing publications on borehole investigations on rock glaciers^{16,28,34} amongst others. The profiles are drawn on the basis of data from the Murtél borehole

viscosity of the shear horizon material has been estimated to be up to seven times smaller than that of pure ice at similar thermal and stress conditions.^{17,48}

In summary, the contribution of the shear horizon to the total surface displacement is large (60%-90%) and it also accounts for most of the inter-annual and seasonal variations in rock glacier creep.^{8,16} Field and theoretical studies^{8,17,18} show that at temporal scales from months to several years, these variations are mainly controlled by pore water pressure within the shear horizon. At longer temporal scales, changes in the structure of the shear horizon, driven by the combined

influence of permafrost creep and ground temperature, are still poorly understood but are expected to play an important role in determining the long-term evolution of rock glaciers and their dynamics.^{4,6,49}

3 | THE DEFINITION OF THE BULK CREEP FACTOR

Developing a mathematical formulation of a natural system - a model - can be used to study its properties and understand its dynamics. All

models have to be constrained and validated with observations, regardless if they are based on statistical methods or on analytical formulations of physical processes. In comparison to glaciology, where copious studies have investigated the physics of ice, research on rock glaciers is characterised by a paucity of direct investigations both in the field and in the laboratory. This limitation restrains our understanding of the fundamental processes governing rock glacier creep and hinders the establishment of quantitative models for investigating rock glacier dynamics. The growing interest in rock glacier dynamics, in combination with increasing data available from remote sensing techniques, attest the need for a comprehensive description of rock glacier creep. Having in mind the most important findings on the physics of rock glacier creep outlined in the previous section, we now formulate them mathematically. Thereafter, we investigate the relationship between rock glacier thickness, surface slope and creep rates for a set of 28 rock glaciers worldwide for which such data is available. On the basis of this analysis, we introduce the Bulk Creep Factor (BCF) and its physical interpretation.

3.1 | Rheological models

The rheology of debris-ice mixtures, i.e. the mechanical constitutive relationship which combines the deformation of the material to its internal stresses, can be described mathematically. Having identified ice creep as the main mechanism behind the movement of rock glaciers, the first theory to consider when describing rock glacier deformation is the empirical flow law proposed by Nye⁵⁰ and Glen⁵¹ for pure ice:

$$\dot{\gamma} = A\tau^n. \quad (1)$$

Glen's law describes thermally activated dislocation creep for an isotropic crystalline solid and is analogous to the relationships that describe deformation of metal and rock at high temperatures.⁵² The shear strain rate $\dot{\gamma}$ depends solely on the shear stress τ through a power law relationship, and on the constitutive properties of clean ice, which are described through two parameters: the fluidity factor A (inversely related to viscosity) and the flow exponent n . The fluidity parameter in equation 1 is described by an Arrhenius relation dependent on temperature:⁵³

$$A = A_0 \exp\left(-\frac{Q}{R_* T}\right), \quad (2)$$

where A_0 is a parameter typical of the material, Q is the activation energy, R_* is the universal gas constant and T is the absolute temperature in Kelvin. This formulation has been proven valid for most glacial and periglacial conditions on earth.²⁵ When approaching the melting point, the fluidity parameter shows an additional dependence on temperature due to liquid water along grain boundaries.^{25,54} This effect can be accounted for by correcting the formulation of the fluidity parameter (Equation (2)) with an additional term:

$$A' = A + \alpha w_w, \quad (3)$$

where w_w is the unfrozen volumetric water content and α a parameter.⁵⁵ The flow exponent n is often considered constant and best approximated for pure ice by a value of 3, although experimental and field evidence exist that this value represents the superposition of different mechanisms.^{52,55}

The previous theory has to be expanded when studying rock glaciers. In fact, they consist of debris-ice mixtures, whose properties depend on the volumetric fractions of their constituents and not only on pore ice. For a rock glacier, the driving stress can be calculated as:

$$\tau = \rho g H \sin \alpha, \quad (4)$$

where g is the gravitational acceleration, H the thickness of the moving rock glacier, α the surface slope angle and ρ is the density of the creeping material, which is given by the contribution of volumetric debris w_d and ice content w_i and the relative densities ($\rho_i = 910 \text{ kg m}^{-3}$ and $\rho_d = 2700 \text{ kg m}^{-3}$):

$$\rho = \rho_d w_d + \rho_i w_i. \quad (5)$$

As we have seen above, several field observations, integrated by theoretical and experimental studies, have highlighted debris concentration and size, temperature, water content and internal stresses as the first-order variables governing the deformation of debris-ice mixtures.²⁵ Arenson and Springman⁵⁶ have tested natural (from borehole cores at rock glacier sites in Switzerland) and synthetic soil samples in order to adapt Glen's flow law to the rheology of rock glacier material.³⁰ The authors expressed the dependency on the volumetric ice content w_i by introducing a logarithmic term to equation 2 and a linear dependency to the flow exponent:

$$A = \exp\left(\frac{a}{1+w_i}\right) + 5 \times 10^{-11} e^{-10.2w_i}, \quad (6)$$

$$n = 3w_i. \quad (7)$$

In addition to the variability of material properties, also the processes governing the deformation of rock glaciers can be diverse. For debris-ice mixtures with a high volumetric content of debris, frictional effects ensue when particle to particle contact is reached. For the end-member case of unfrozen debris, the maximum strength is in first approximation described by the Terzaghi form of the Mohr-Coulomb yield criterion:

$$\tau_r = \tau_{c\theta} + \sigma_e \tan \phi_c, \quad (8)$$

where σ_e are the effective stresses, $\tau_{c\theta}$ is the cohesion and ϕ_c is the friction angle of the shear horizon material. Contrarily to unfrozen material, the strength of ice-rich debris is strongly strain rate and temperature dependent and preserves a viscous component due to the presence of pore ice. Ladanyi⁵⁷ has proposed a constitutive relation

that combines the frictional yield threshold with viscous flow resistance. In this mathematical formulation, the shear strain rate depends on the shear stress and on two creep parameters, and additionally on the shear resistance of the deforming material. For an ice-rich, cold frozen soil, where both cohesion and friction are affected by temperature and strain rate, the shear strain rate becomes:

$$\dot{\gamma} = \dot{\gamma}_c \left(\frac{\tau}{\tau_r} \right)^n, \quad (9)$$

where $\dot{\gamma}_c$ is the critical shear strain rate typical of the material. This formulation allows to express the frictional behaviour of the ice-rich mixture augmented by a rate-dependent cohesive strength. Moreover, according to the definition of the shear strength, we are able to consider the effect of pore water pressure on the driving stress through the calculation of the effective stresses σ_e .

3.2 | Rock glacier thickness and driving stress

While it is relatively simple to determine the surface slope and the displacement rates of rock glaciers, inferring information about their thickness remains challenging. Geophysical methods such as electrical resistivity tomography (ERT), seismic and ground penetrating radar surveys (GPR) allow the investigation of ground permafrost at depth. However, using such indirect observations to infer the thickness of the moving rock glacier remains laborious and often impossible due to practical reasons. Boreholes instrumented with slope inclinometers provide the most reliable results with this regard, but this information is only punctual and they are expensive both logistically and financially. For all of the above, the application of inverse models for the derivation of rock glacier thickness is desirable. Contrarily to ice-glaciers, where several methods have been proposed and their limitations critically reviewed and evaluated,⁵⁸ no detailed studies of such methods have been undertaken for rock glaciers. Therefore, we propose three approaches to estimate rock glacier thickness based on the analysis of a dataset of 28 rock glaciers from the Alps (23) and the Andes (5), for which detailed observations of surface creep rates, slope angle and thickness from different sources are available. Detailed information about the dataset and the relative bibliography is available in supporting information.

In Figure 3 we analyse the thickness, driving stress, creep rates and slope angles for the investigated dataset. The distribution of thickness and driving stresses (calculated according to Equation (4)) for the analysed rock glaciers suggests a visco-plastic behaviour with a yield stress of about 100 kPa, similar to clean ice (Figure 3a). When considering all the rock glaciers in the dataset, the average driving stress is 85 ± 21 kPa. However, a cluster of five rock glaciers in the Chilean Andes shows low values of the driving stress. These landforms are in degrading conditions (with permafrost temperatures being at 0°C) and their driving stresses might not be able to sustain steady state creep conditions any longer. When excluding these five degrading rock glaciers from the analysis, the mean value of the driving stress increases up to 92 ± 13 kPa. This result confirms and

extends previous observations by Wahrhafting and Cox² and Whalley and Martin,⁵⁹ which performed a similar analysis on a vast dataset of rock glaciers finding that the driving stresses vary between 50 kPa and 200 kPa. Note that in these previous studies the thickness was generally estimated on the basis of expeditious field surveys subject to larger uncertainties.

The distribution of rock glacier thickness and surface slope angle is shown in Figure 3b along with three model fits and their performance, which is quantified with the RMSE. The first method that we propose to estimate the thickness of a rock glacier is a constant model. This approach is supported by the fact that while most of the observed rock glaciers present a thickness of their moving part between 10 m and 30 m, only few rock glaciers have been studied in such detail that the uncertainty on the estimation of the thickness is limited to less than the natural variability between different landforms. When fitting the constant model to the analysed dataset, the mean value of rock glacier thickness becomes:

$$H = 20 \pm 5.5\text{m}. \quad (10)$$

The second model to estimate rock glacier thickness is a linear relationship between slope angle and thickness. From the available observations, we find a best linear fit of:

$$H = 37 - 0.9\alpha \pm 3.0\text{m}. \quad (11)$$

The third model, also used in the field of glaciology, estimates the thickness of the rock glacier with a perfectly plastic model by solving Equation (4) for H , assuming a yield stress of $\tau = 92$ kPa (given the mean driving stress from the dataset):

$$H = \frac{\tau}{\rho g \sin \alpha} \pm 3.4\text{m}. \quad (12)$$

According to our results, the linear thickness model shows the best performance (RMSE = 3.0 m), but is only marginally better than the plastic model (RMSE = 3.4 m). Note that the suggested models should be applied with caution and only in average slope ranges roughly between 10° and 30° of slope (i.e. for the slope angle range in which they have been derived from the data).

Rock glacier creep rates can be calculated by coupling one of the thickness models (Equation (10), 11 or 12) to the creep models presented in Section 3 (Equation (1) or Equation (9)). Figure 3c shows the result of this coupling and demonstrates that the choice of the thickness model has a strong influence on calculated creep rates. When coupling the linear and the plastic thickness models to Glen's flow law, the creep rates decrease for high values of the slope angle. This mathematical artefact originates from the vertical integration of Equation (1). In fact, the creep rates are proportional to the thickness to the power of $n + 1$, which in turn is (in the suggested thickness models) inversely proportional to the slope angle. This artefact can be overcome by coupling the thickness models to the creep model of Ladanyi.⁵⁷ In this case (Equation (9)), the shear rates show a linear

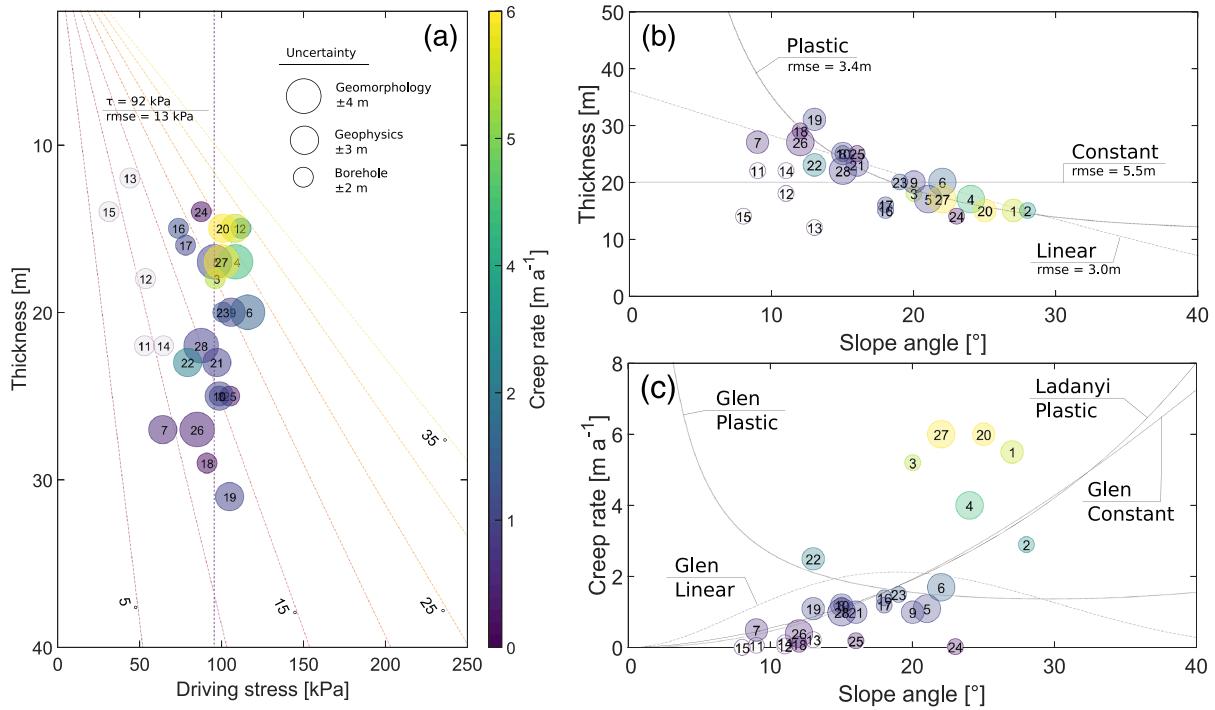


FIGURE 3 Analysis of observed rock glacier thickness, slope angle, and creep rates. Each rock glacier is depicted by a circle, whose colour represents the rock glacier creep rates [ma^{-1}] as indicated by the colour bar. For each rock glacier, the uncertainty relative to its thickness is represented by the diameter of the circles. (a) Rock glacier thickness [m] against driving stress [kPa]. The vertical dashed line shows the average value of the driving stress and the relative RMSE. The diagonal dashed lines show constant values of the slope angle, from 5° to 35° . (b) Rock glacier thickness [m] against slope angle $^\circ$. The three models to calculate rock glacier thickness are indicated by labelled lines along with their RMSE. (c) Rock glacier creep rates [ma^{-1}] against slope angle $^\circ$. The four models for the calculation of rock glacier creep rates are shown. The corresponding labels indicate from top to bottom the respective creep and the thickness models used for the calculation

dependency on the thickness and depend on the surface slope angle to the power of n , which therefore dominates the equation. A similar dependency on the slope angle is obtained when combining Glen's flow law with the constant model for rock glacier thickness, i.e. only accounting for variations in the slope angle and substantially neglecting changes in the rock glacier thickness. Although the last two mentioned combinations (constant thickness + Glen and plastic thickness + Ladanyi) provide similar results, we prefer the second approach because it represents the observed thickness dependency on slope more realistically (Figure 3b).

After the above analyses, we can conclude that (i) the typical driving stress of alpine rock glaciers is 92 ± 13 kPa suggesting a plastic behaviour, (ii) the thickness of the moving part of a rock glacier can be estimated with the use of simple models on the basis of the surface slope angle, (iii) surface creep velocities can be described on the basis of surface slope observations and thickness models in combination with a creep law - preferably accounting for the frictional behaviour of rock glacier creep.

3.3 | The Bulk Creep Factor BCF and its physical interpretation

A complete description of rock glacier dynamics is hampered by the high degree of heterogeneity of their physical properties in

conjunction with the strenuousness to obtain accurate measurements of their internal structure, especially at a regional scale.¹⁹ In an attempt to better understand regional patterns and tendencies, we describe rock glacier creep and dynamics with the most simple method possible, seeking a compromise between a gargantuan task and its complete omission.

Based on the brief review on rock glacier physics and its mathematical description presented in the previous sections, we define the Bulk Creep Factor (here on BCF) as the ratio between observed c_{obs} and modelled c_{mod} creep rates:

$$BCF = \frac{c_{obs}}{c_{mod}} \tag{13}$$

Following the analysis presented in Section 3.2, we adopt the creep model proposed by Ladanyi⁵⁷ and calculate rock glacier creep rates by integrating Equation (9) in the vertical dimension and obtain:

$$c_{mod} = \frac{\dot{\gamma}_c}{n+1} \left(\frac{\rho g \sin \alpha}{\tau_{c0} + \rho g H \cos \alpha \tan \phi} \right)^n H^{n+1} \tag{14}$$

Combining this equation to Equation 13, the BCF becomes:

$$BCF = c_{obs} \frac{(n+1)}{\dot{\gamma}_c} \left(\frac{\tau_{c0} + \rho g H \cos \alpha \tan \phi}{\rho g \sin \alpha} \right)^n H^{-(n+1)}. \quad (15)$$

The BCF is a dimensionless quantity that expresses the mechanical properties of the rock glacier material. By separating the geometrical influence from the creep rates, the BCF allows to compare different rock glaciers or different areas of a single rock glacier with regard to their rheological properties. As we did not distinguish between different layers in the vertical integration of Equation (9), the BCF implicitly describes the rheology of both the ice-rich core and the shear horizon. It therefore represents an averaged value over the entire rock glacier thickness. In order to overcome our limited knowledge about the internal structure of rock glaciers, we evaluate the value of the thickness H with one of the thickness models proposed in the previous section (Equation (10) to Equation (12)). This approach has the great advantage of requiring only remote sensing data of surface creep velocities and surface slope angles of the rock glaciers. Therefore, it allows large scale applications to efficiently extend previous research efforts.^{59,60} Here on, we set the values of the model parameters according to previous modelling and laboratory experiments.^{5,6,8,25,56,61} While most of the parameters are well constrained and can be parametrised (e.g. as a function of the volumetric ice content), the value of $\dot{\gamma}_c$ varies between different rock glaciers and the choice of a reference value is arbitrary. We calibrate this parameter to 0.06 a^{-1} in order to reflect the velocities of the Murtél Rock Glacier (and most of the rock glaciers analysed in this study). This value is thus taken as a regional reference for our analysis. While this reference is arbitrary and the absolute values of the BCF can change, it does not influence the relative variation between different rock glaciers.

When adopting the perfect plastic model for rock glacier thickness (Equation (12), with a yield stress of 100 kPa) and assuming standard values of the material parameters ($w_i = 0.7$, $n = 2.1$, $\rho = 1500 \text{ kg m}^{-3}$, $\phi = 25^\circ$, $\tau_{c0} = 10 \text{ kPa}$, and $\dot{\gamma}_c = 0.06 \text{ a}^{-1}$), the formulation of the BCF simplifies to:

$$BCF = 7.6 c_{obs} \sin \alpha \left(\frac{0.5}{\tan \alpha} + 0.1 \right)^{2.1} \quad (16)$$

Figure 4a shows the procedure and the data required for the calculation of the BCF. The interpretation of different values of the BCF are illustrated in Figure 4b. Here, three possible states of a rock glacier are depicted in the creep rate - surface slope angle space. One rock glacier can be described by a single point under the assumption that the spatial variability within the same landform can be represented by single values of the surface slope angles, thickness and creep rates. Point A and point C represent two rock glaciers characterised by the same rheological properties (both lay on the yellow contour line - high BCF), but show very different creep rates due to their contrasting slope angles. Point A and point B on the contrary, show rock glaciers with the same value of creep rates despite their difference in geometry (surface slope angle). This is only possible due to a reduction of the BCF. The rock glaciers visualised by point B and point C show the

same value of the slope angle, but different values of creep rates due to different mechanical properties (different BCF). This illustration demonstrates the importance of accounting for geometry and material properties when comparing rock glacier dynamics. In fact, on a kinematic level, point A and point B are equivalent. However, our approach allows to illustrate the dynamic difference between those two rock glaciers: if point A had the same slope as point B, it would creep four times faster according to its rheological properties.

4 | APPLICATIONS: RHEOLOGICAL INFORMATION FROM REMOTE SENSING DATA

In the following, we illustrate two possible applications of the proposed methodology for investigating rock glacier dynamics. At a regional scale, we analyse a large dataset of rock glaciers from the Alps to investigate their dynamical behaviour. At a local scale, we use detailed observations of the surface creep velocities of three rock glaciers to analyse their spatial variability.

4.1 | The regional scale: a dynamic comparison of alpine rock glaciers

Many efforts in the context of national and international permafrost monitoring are directed towards the assessment of rock glacier surface displacements at both local and regional scale.^{60,62-65} In most studies that analysed surface velocities so far, different rock glaciers are compared on the basis of kinematic data only, despite their contrasting geometrical settings. The introduction of the BCF allows to include information about their thickness and surface slope, thus to transpose the analysis from a kinematic to a dynamic level.

For our analysis at a regional scale, the spatially heterogeneous characteristics of a rock glacier are summarised by a single value of the BCF, which is in first approximation representative for the entire landform (or a substantial part of it). The proposed approach can thus be applied to analyse data on surface slope and surface displacements obtained from in-situ or remote sensing techniques. We investigate here a dataset comprising 414 rock glaciers for which surface displacement and slope angle data are available. The majority of the data come from an analysis of the French national inventory.⁶⁶ Other data points come from the Swiss,^{65,67} Austrian⁶⁰ and Italian Alps. In a first step, we calculate and analyse the BCF for all rock glaciers in the dataset. In a second step, we explore the influence of permafrost conditions at each rock glacier site by using as a proxy the Permafrost Zonation Index (PZI) developed by the University of Zurich.⁶⁸ High values (close to the unit) correspond to favourable conditions for permafrost occurrence, while values close to zero indicate unfavourable conditions. Moreover, we analyse the destabilization susceptibility of the investigated rock glaciers according to the geomorphological index proposed by Marcer et al.⁶⁴ For a more detailed description of the dataset we refer to Table 2 in the supporting information.

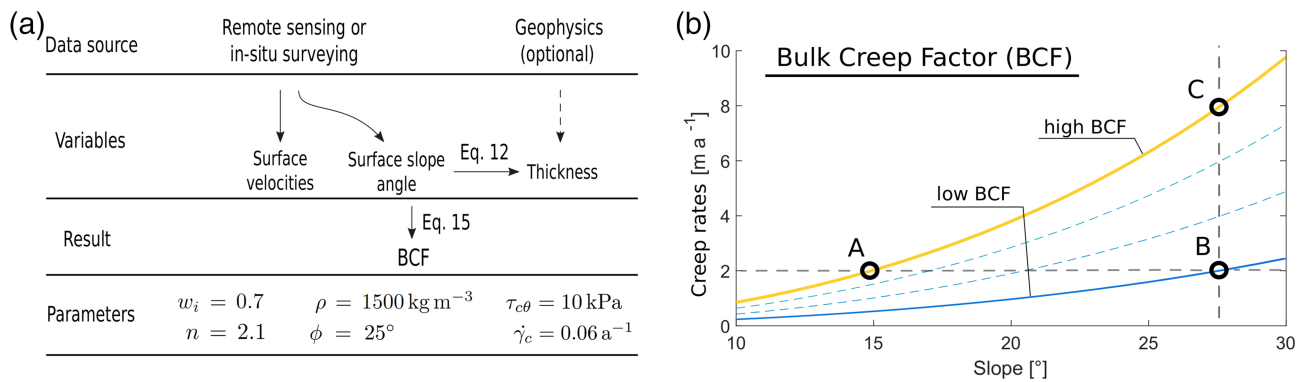


FIGURE 4 Calculation and interpretation of the BCF. (a) Procedure and data required for the calculation of the BCF and (b) interpretation of the parameter values in the creep rates - slope angle space. The coloured contour lines show constant values of the BCF. The interpretation is presented in the text

Figure 5 shows the results of the BCF in relation to dynamics and geometry for all 414 rock glaciers in the dataset. The sub-figures visualize the relation between surface creep rates, surface slope angle, BCF and PZI in different combinations. Circular and diamond markers indicate active and destabilised rock glaciers respectively, according to the criteria from Marcer et al.⁶⁴ Most rock glaciers show a surface slope comprised between 10° and 35° , surface creep rates lower than about 2 m a^{-1} and exhibit a BCF lower than 5 (70% of the rock glaciers in the dataset). Almost only destabilised rock glaciers or rock glaciers with low PZI have high BCFs as shown in Figure 5b-d.

As we have presented above, the calculation of the BCF expresses the rheological properties of the rock glacier material by removing the geometrical information from the velocity signal and thereby allows the comparison of the dynamical behaviour of different rock glaciers. Figure 5a and b confirm that the material properties (BCF) and the surface slope angle are independent (if we exclude feedback between shear rates and material structure), while the surface velocities depend with a power law on the surface slope. In the slope-velocity space in Figure 5a the maximum creep rate observed increases with the slope angle: e.g. all the rock glaciers with velocities above 4 m a^{-1} are characterised by slope values higher than 25° . Nevertheless, there are also rock glaciers with low values of creep rates regardless of their slope angle. The calculated BCFs displayed in Figure 5b reveal how rock glaciers with gentle slope can exhibit material properties prone to fast deformation (high BCFs). For example the Reichenkar Rock Glacier has a similar BCF to the Pierre Brune Rock Glacier despite reaching only half of its creep rates: this discrepancy in creep velocities can be explained by the difference in surface slope. Comparing relative velocity variations is of advantage, but this approach only introduces a linear trend and remain at a kinematical level, still neglecting geometrical and mechanical properties of the rock glaciers.

Figure 5c depicts the relation between BCF, surface slope angle and creep rates. Given a value of the BCF, a wide range of possible velocities can be found, and vice-versa. The value of the surface creep velocity of a rock glacier is fully determined when incorporating the information about the geometry, which is mostly controlled by the surface slope angle. All the rock glaciers are constrained in a sector of

the quadrant bounded by two lines representing the maximum and the minimum surface slope angles of the rock glaciers in our inventory (10° and 30°).

The potential influence of external factors on the BCF is analysed in Figure 5d using the PZI as a proxy for permafrost conditions and temperature. We find that the maximum value of the BCF is delimited by the PZI: for favourable permafrost conditions (PZI close to 1) only small BCF are observed whereas for unfavourable conditions (PZI close to 0) the whole range of low to high BCF occurs. This pattern is consistent with the dual influence of temperature on rock glacier dynamics. Firstly, in the early stage of permafrost degradation, increasing ground temperatures and water content (corresponding to a decrease in the PZI) enhance the deformation (increasing BCF) according to Equation (2) and Equation (3). Secondly, in the final stage of degradation when substantial thawing occurs, the BCF decreases due to lower stresses and enhanced inter-particle friction. Rock glaciers currently experiencing a destabilization process are characterised by high values of the BCF and tend to the limiting line in Figure 5d. Because destabilization is an irreversible process, and degrading rock glaciers that are in the final stage of destabilization can still be classified as such, they drift towards low values of the BCF and PZI. This result implies that a classification of the dynamic state of rock glaciers might be possible on the basis of a combination of PZI, BCF and creep rates. Whereas low PZIs are in general related to unfavourable permafrost conditions, they can indicate current destabilization if occurring together with high BCFs. High values of the PZI indicate active rock glaciers in cold conditions, apparently less likely to destabilize. However, open questions remain and a classification of rock glaciers based on those parameters remains non trivial and requires additional detailed studies.

4.2 | The local scale: Analysing spatial variability in rock glacier creep

For many rock glaciers worldwide, detailed spatial information about the surface topography and their displacement field are becoming available.^{14,15,69,70} The BCF allows to interpret and investigate the

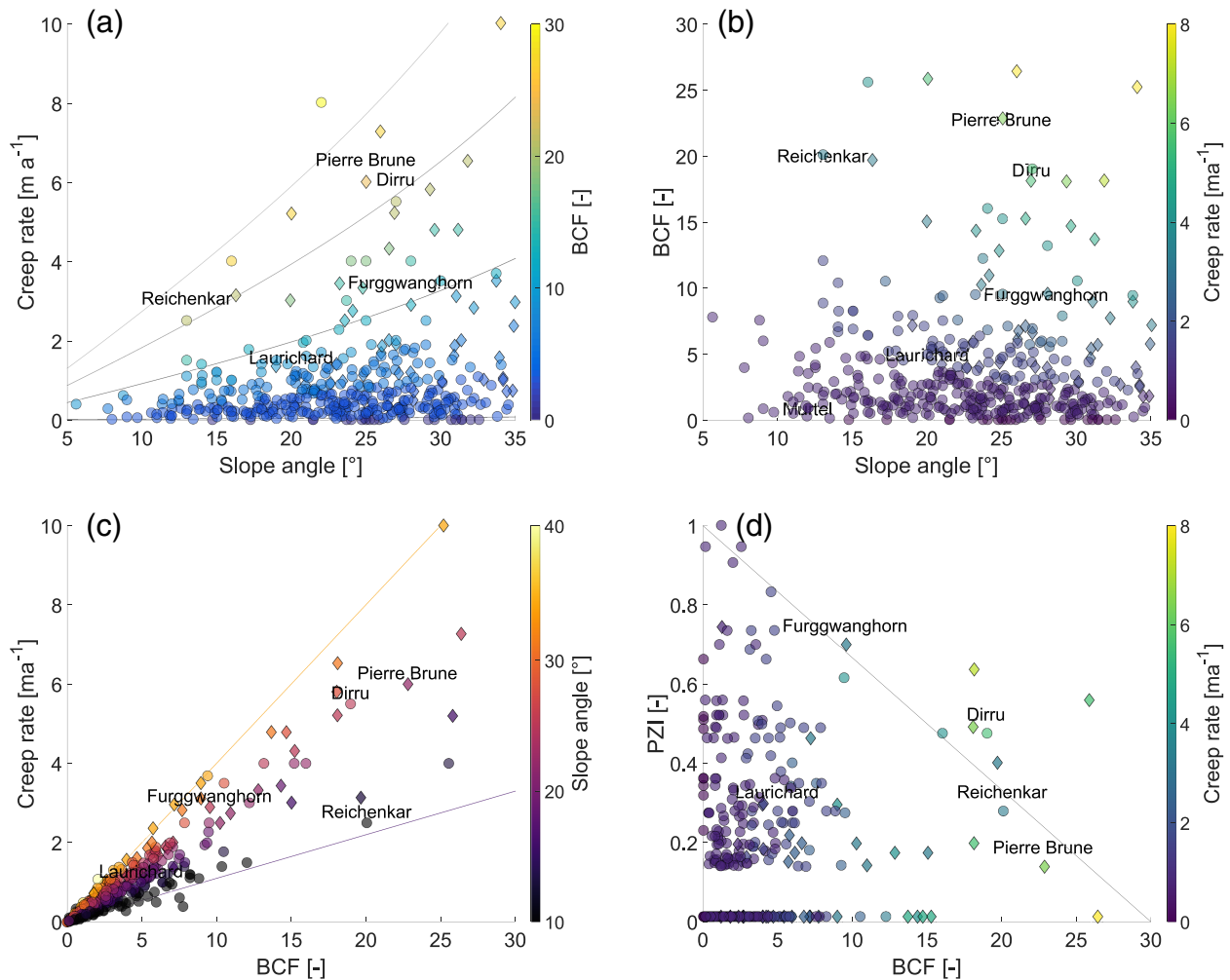


FIGURE 5 Results of the analysis at the regional scale. Each point represents a rock glacier. Destabilised landforms, according to Marcet et al.,⁶⁴ are illustrated with a diamond shape. (a) Surface creep rate against slope angle, (b) BCF against slope angle, (c) creep rate against BCF and (d) PZI against BCF. Additional information about creep rates, BCF or slope angle is provided by the corresponding colour bar

dynamics and mechanical properties of rock glaciers for which such topographic and kinematic information are available. We investigate three rock glaciers characterised by contrasting dynamical states: steady-state creep conditions (Laurichard, FR), exceptionally fast flow (Dirru, CH), and ongoing destabilization (Pierre Brune, FR). For all three study sites detailed digital surface models and surface velocity fields are available from different sources and at different resolutions.

The results of the analysis at the local scale are illustrated in Figure 6. For the Dirru and Pierre Brune Rock Glaciers, the spatial data coverage with regard to creep velocities is almost complete. For the Laurichard Rock Glacier no velocity data is available in the area close to the rooting zone. The observed velocities show two distinctly different patterns of terrain topography and creep rates at the three field sites. For the Laurichard Rock Glacier, the highest velocities are observed in the uppermost area, whereas for the other two the largest values can be observed closer to the front. The three rock glaciers are characterised by velocity values varying between 1 m a^{-1} and 6 m a^{-1} and relatively high values of the slope angle, with values peaking at more than 30° . The uncertainty related to the spatial variability in

velocity is limited in all cases except for a limited area close to the front of the Dirru Rock Glacier.^{71,72} This uncertainty is caused by low performance of the feature tracking algorithm in this area as visible in the corresponding map. The observed field of surface slope angle and surface velocity are smoothed with a Gaussian filter (radius 10 m) in order to reduce undesirable effects of micro-topography on the analysis. On the basis of the values of the surface slope angle, we invert the thickness of the moving rock glacier assuming a yield stress equal to 92 kPa. Narrow peaks and troughs in the thickness profiles correspond to low slope angles due to small-scale undulations of the surface topography (e.g. furrow and ridges).

For the Laurichard Rock Glacier, the calculated BCF remains constant along the investigated profile, despite substantial variations in slope angle and creep rates. The average value of the BCF is 5 (as also visible in Figure 5), confirming its validity as a reference rock glacier for the Alps.

For the Dirru Rock Glacier the analysed profile extends from the steep front up to the rooting zone. Here, despite strong variations in geometry and the possible influence of 2D effects and the acute

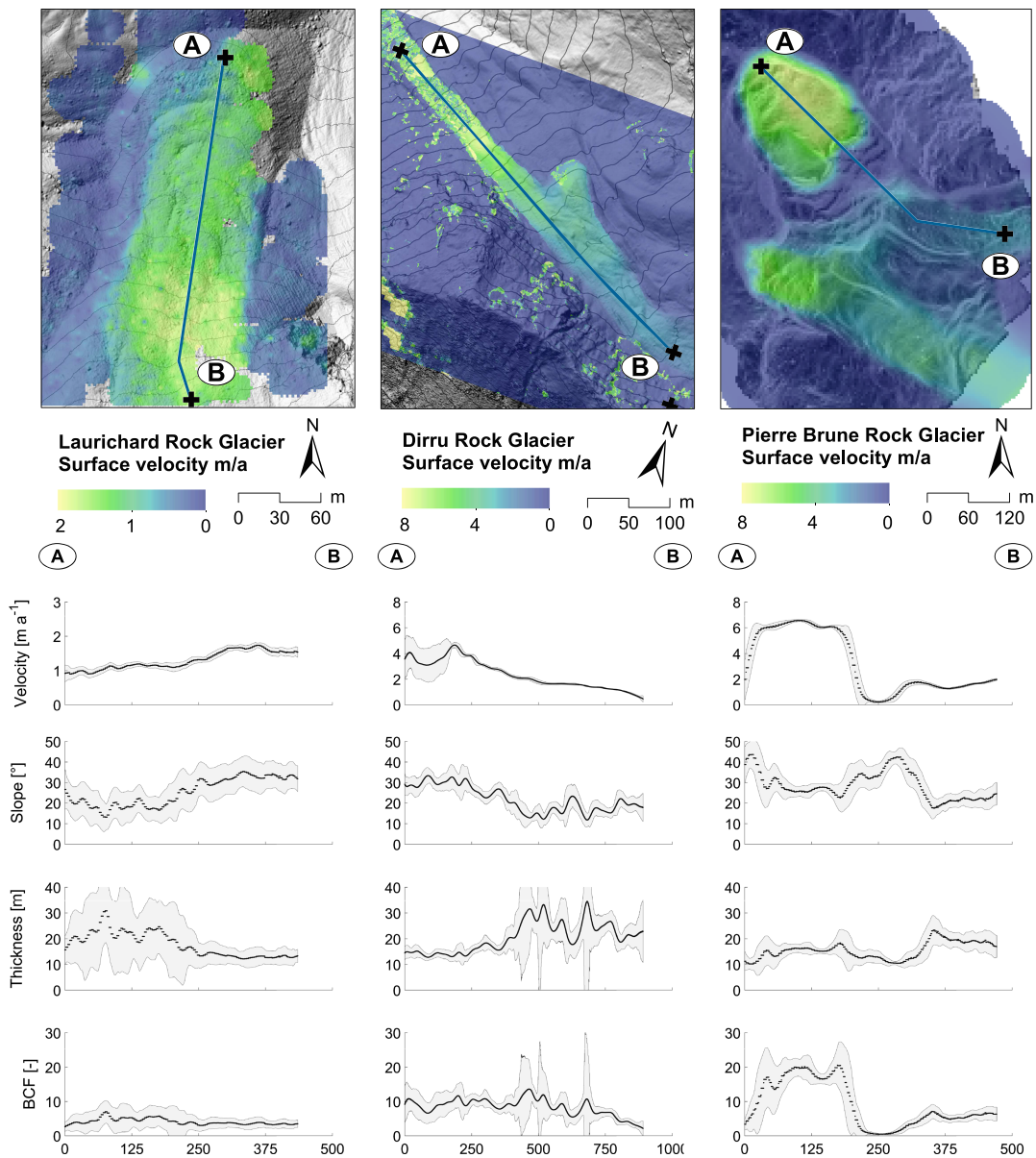


FIGURE 6 Results at local scale. From left to right, Laurichard, Dirru and Pierre Brune Rock Glaciers. The the upper panel shows the surface creep velocities (colour coded) together with the profile along which the analysis is performed: from A the front to B the rooting zone. Below, from the top to the bottom, the observed surface velocities, surface slope angles, modelled thickness and BCF are plotted along the corresponding profiles. The shaded gray area depicts the spatial variability of the plotted variable in an area of 25 m along each position and can be used as a proxy for the uncertainty of the results

change in slope, the BCF is almost constant along the entire profile, with the exception of the rooting zone where it decreases substantially. Similarly to the case of the Laurichard Rock Glacier, the constant value of the BCF shows that the spatial variations in creep rates can be explained by geometry (slope and thickness). The average value of the BCF = 10, coherent with the value at the regional scale (Figure 5), indicates a predisposition to high creep rates along the entire profile.

The Pierre Brune Rock Glacier on the contrary shows a distinctly different pattern in BCF. In this case, the topography cannot account for the large variations in surface creep rates along the profile. Close to the front, where the highest rates are observed, the BCF exceeds

values of 20. In the upper section, the BCF is four times smaller than close to the front. In the center corresponding to a scarp-area,⁶⁴ the velocities are almost zero despite the large values of the slope angle. As a consequence the BCF shows very low values, confirming on the one hand the dynamic separation between the lowermost and the uppermost unit and on the other hand indicating degrading conditions in the scarp area.

According to the results of our analysis, the spatial variability in surface velocity between the upper and the lower part for the Laurichard and the Dirru Rock Glacier can be explained by their geometry (surface slope and thickness) alone. In this sense, the two rock glaciers can be considered similar, both showing a constant value

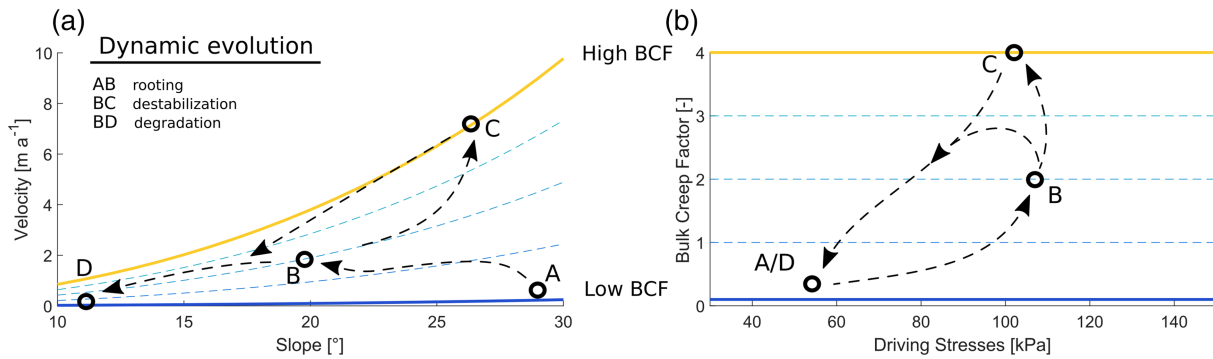


FIGURE 7 Schematic representation of possible dynamical evolution (indicated by the dashed arrows) of a rock glacier in the (a) velocity-slope and in the (b) BCF-driving stress space. The points represent possible combination of variables for (A) rooting, (B) secondary creep, (C) destabilization, and (D) degradation conditions. The values are indicative of typical conditions for alpine rock glaciers

of the BCF, consistent to the analysis at the regional scale in the previous section. However, the contrasting values of the BCF between the two rock glaciers indicate rheological differences that reflect profound diversity in material properties. Further interpretation requires analysis based on detailed in-situ observations (e.g. surface or ground temperature measurements, geophysical surveying, etc.). For the Pierre Brune Rock Glacier the velocity distribution can be explained only by accounting for both the geometry and the strong spatial discontinuity in the BCF between the upper and the lower part. The discontinuity in the BCF and its exceptionally high values point towards a dynamical and rheological interpretation of the destabilization phenomenon confirming and complementing geomorphological and kinematic observations as seen in the analysis at the regional scale (Section 4.1).

5 | THE LONG-TERM DYNAMIC EVOLUTION OF ROCK GLACIERS

The BCF can further be applied to interpret and investigate the evolution of rock glacier dynamics over longer time scales as illustrated in Figure 7. This figure illustrates the possible dynamical evolution of a rock glacier in a Lagrangian reference system (following an individual point in space and time as it creeps). In Figure 7 we can follow the evolution of a material point on the surface of a rock glacier based on its surface slope and velocity; in Figure 7b we can follow the evolution of the same point by looking at its BCF and the corresponding driving stress.

The evolution of a rock glacier during its rooting from a talus slope is depicted by line (I) moving from point A to point B. Here, the slope is significantly decreasing from the steeper zone of the talus to the more gentle areas below, while the Bulk Creep Factor is increasing due to the initiation of the creeping process (towards point B). Lines II and III show the dynamic evolution of a rock glacier experiencing destabilization. When the front of the rock glacier reaches a steeper terrain it moves faster, but maintains its physical properties for a determined period of time, therefore moving along an isoline in the two figures. When destabilization occurs due to topographical

predisposition and permafrost temperatures approaching the melting point, the Bulk Creep Factor drastically increases causing a diversion of the trajectories from the isoline until point C where the highest velocities are reached. Currently in the Alps there is an increasing number of rock glaciers following this path (line II), e.g. the Tsarminne and the Pierre Brune rock glaciers.^{10,73} From point C onward (line III), the rock glacier continues to creep with decreasing but still relatively high velocities due to a change in surface slope or due to permafrost degradation. Permafrost thawing causes the driving stress to decrease and the density of the rock glacier approaches the maximum packing density while interlocking becomes more important. Eventually creep ceases and the dynamic evolution of the rock glacier comes to an end with its transitions from an active to an inactive state (line IV). Two mechanical effects may independently lead to the deactivation of the rock glacier: the decrease in stresses, which is driven by decreasing thickness and surface slope, and the decrease in the BCF (see Barsch⁷⁴ for a geomorphological interpretation). Examples of well studied rock glaciers currently in such condition are the Furgwannghorn and Tête de Longet rock glaciers.^{10,18} Line III and line IV represent the degradation process, which can vary its trajectory depending on the different starting condition (C - destabilization or B - secondary creep). Starting from a secondary creep phase, degradation still causes the driving stresses to decrease but initially leads to an acceleration due to permafrost warming and therefore an increase in the BCF (line IV). Many rock glaciers in the Alps currently find themselves in this condition with temperatures approaching the melting point, increasing velocity and onset of degradation.⁶⁵ The positions A and D coincide in Figure 7b, sharing low stresses and a low BCFs. The exact position of the two points in the figure depends on the rock glacier structure and on the terrain topography.

6 | CONCLUSIONS

Based on a brief review of the physics of rock glacier creep and the mathematical formulation used to describe it, we have presented a general theory of rock glacier creep and have introduced the Bulk Creep Factor as a measure of the rheological properties of rock

glaciers. The proposed approach only requires data on creep velocities and slope angle, which both can be derived operationally over large areas from remote sensing data (or from detailed in-situ measurements). Therefore, the BCF has a large potential for investigating the dynamic state and rheology of large scale rock glacier datasets. Additionally, we have provided two examples of possible applications of the BCF at a regional and at a local scale. The combined analysis at both scales indicates the potential of the BCF to evaluate and compare the state of rock glacier dynamics from remotely sensed data.

With regard to limitations: the proposed theory shows two main weaknesses. On the one hand, it relies on the combination of two different rheologies for the determination of the thickness and the rheological properties of the rock glacier material. This point can be overcome by direct measurements of rock glacier thickness or by the application of dynamical models. On the other hand, the BCF neglects in first approximation the vertical structures of rock glaciers and the differences between the shear horizon and the ice-rich core. More field observations and modelling studies are still needed in order to better constrain this diversity and in order to transpose it to analyses at a regional scale. Concluding, the main findings of this study can be summarised as follows:

- Remote sensing data in combination with mathematical formulations can be used to analyse rock glacier dynamics at a regional and at a local scale.
- The typical driving stress of alpine rock glaciers is 92 ± 13 kPa.
- Rock glacier thickness can be efficiently estimated with the inversion of simple models (e.g. perfectly plastic model), but more detailed data is needed for further validation of this approach.
- Rock glacier creep rates can be calculated by coupling a rheological model accounting for the frictional behaviour of rock glacier creep to a perfectly plastic model for rock glacier thickness.
- The introduction of the Bulk Creep Factor allows the physical interpretation of the rheological properties of the constitutive material and the processes controlling rock glacier creep by separating the geometry information from the velocity signal.
- Most alpine rock glaciers show a BCF lower than 5.
- First order variables controlling the BCF are temperature and water content. Further observational data are required to better constrain their influence.
- Only rock glaciers experiencing destabilization or set in conditions unfavourable to permafrost occurrence show large values of the BCF, with maximum values close to 20.
- The permafrost conditions (approximated here by the PZI) define a maximum limit for the BCF.
- For dynamically non-destabilized rock glaciers, the geometry can explain the spatial variability in creep rates with almost constant rheological properties of the constitutive material.
- Destabilised rock glaciers are characterised by contrasting and discontinuous material properties (BCF). In addition to geomorphological observations, the definition of rock glacier destabilization should account for the rheological and dynamical state of the rock glacier rather than solely on its kinematics.

This study represents a first attempt to investigate in detail the spatial variability and the large scale patterns and trends of rock glacier dynamics. The concept of the BCF seems very promising and has the potential for further and wide spread applications. However, more research is needed and additional data must be collected in order to validate and increase the confidence in the proposed theory. In a next step the BCF should be further analysed in relation to the factors influencing it (e.g. thermal state, liquid water, internal structure...) and the modelling-approach be better constraint with more detailed observations at longer time series.

ACKNOWLEDGEMENT

This research was part of the project X-Sense2 and was financed by nano-tera.ch (ref. no. 530659) and the University of Zurich. The authors thank the input from Reynald Delaloye for the data used in both datasets (see supporting information). The authors thank the contribution of J. Beutel for its important contribution to the collection of kinematic data in the Swiss Alps, N. Mölg and C. Rohner for the support in acquiring and analysing the data for Dirru Rock Glacier.

DATA AVAILABILITY STATEMENT

The data used for the analysis of rock glacier thickness and for the application at both regional and local scale are summarised in the supporting information and are available from the authors upon request.

ORCID

Alessandro Cicoira  <https://orcid.org/0000-0002-0065-4464>

Marco Marcer  <https://orcid.org/0000-0002-2749-8051>

Xavier Bodin  <https://orcid.org/0000-0001-6245-4030>

Lukas U. Arenson  <https://orcid.org/0000-0001-7172-6683>

Andreas Vieli  <https://orcid.org/0000-0002-2870-5921>

REFERENCES

1. Capps SR. Rock glaciers in alaska. *J Geology*. 1910;18:359-375.
2. Wahrhaftig C, Cox A. Rock glaciers in the alaska range. *GSA Bull*. 1959;70(4):383.
3. Haeberli W. Creep of mountain permafrost. *Mitteilungen der Versuchsanstalt für Wasserbau, Hydrologie und Glaziologie der ETH Zurich*, vol. 77; 1985.
4. Kaab A, Frauenfelder R, Roer I. On the response of rockglacier creep to surface temperature increase. *Global Planet Change*. 2007;56(1): 172-187.
5. Monnier S, Kinnard C. Interrogating the time and processes of development of the las liebres rock glacier, central chilean andes, using a numerical flow model. *Earth Surface Processes Landforms*. 2016;41(13):1884-1893.
6. Muller J, Vieli A, Gartner-Roer I. Rock glaciers on the run – understanding rock glacier landform evolution and recent changes from numerical flow modeling. *Cryosphere*. 2016;10(6):2865-2886.
7. Cicoira A, Beutel J, Gartner-Roer I, Faillettaz J, Vieli A. Resolving the influence of temperature forcing through heat conduction on rock glacier dynamics a numerical modelling approach. *Cryosphere*. 2019a; 13(3):927-942.
8. Cicoira A, Beutel J, Faillettaz J, Vieli A. Water controls the seasonal rhythm of rock glacier flow. *Earth Planet Sci Lett*. 2019b;528: 115844.

9. Delaloye R, Morard S, Barboux C, et al. Rapidly moving rock glaciers in mattertal. *Jahrestagung Der Schweizerischen Geomorphologischen Gesellschaft*. 2013;29:21-31.
10. Marcer M, Cicoira A, Cusicanqui D, Bodin X, Echelard T, Obregon R, Schoeneich P. Rock glacier destabilization due to climate change. *Nature Communications Earth Environment* submitted.
11. Kaab A, Weber M. Development of transverse ridges on rock glaciers field measurements and laboratory experiments. *Permafrost Periglacial Process*. 2004;15:379-391.
12. Hartl L, Fischer A, Stocker-Waldhuber M, Abermann J. Recent speed-up of an alpine rock glacier an updated chronology of the kinematics of outer hochebenkar rock glacier based on geodetic measurements. *Geografiska Annaler Ser A, Phys Geography*. 2016;98:129-141.
13. Wirz V, Gruber S, Purves RS, et al. Short-term velocity variations at three rock glaciers and their relationship with meteorological conditions. *Earth Surface Dyn*. 2016;4(1):103-123.
14. Bodin X, Thibert E, Sanchez O, Rabatel A, Jaillet S. Multi-annual kinematics of an active rock glacier quantified from very high-resolution DEMs an application-case in the french alps. *Remote Sens*. 2018;10:547.
15. Vivero S, Lambiel C. Monitoring the crisis of a rock glacier with repeated UAV surveys. *Geographica Helvetica*. 2019;74(1):59-69.
16. Arenson L, Hoelzle M, Springman S. Borehole deformation measurements and internal structure of some rock glaciers in Switzerland. *Permafrost Periglacial Process*. 2002;13(2):117-135.
17. Ikeda A, Matsuoka N, Kaab A. Fast deformation of perennially frozen debris in a warm rock glacier in the Swiss Alps an effect of liquid water. *J Geophys Res Earth Surf*. 2008;113(F1):F01021.
18. Buchli T, Kos A, Limpach P, Merz K, Zhou X, Springman S. Kinematic investigations on the Furggwanhorn rock glacier, Switzerland. *Permafrost Periglacial Process*. 2018;29(1):3-20.
19. Arenson L, Kaab A, O'Sullivan A. Detection and analysis of ground deformation in permafrost environments. *Permafrost Periglacial Process*. 2016;27(4):339-351.
20. Olyphant G. Computer simulation of rock-glacier development under viscous and pseudoplastic flow. *GSA Bull*. 1983;94(4):499-505.
21. Jansen F, Hergarten S. Rock glacier dynamics stick-slip motion coupled to hydrology. *Geophys Research Letters*. 2006;33(10):1-4. <https://doi.org/10.1029/2006GL026134>
22. Frehner M, Ling A, Gartner-Roer I. Furrow-and-ridge morphology on rockglaciers explained by gravity-driven buckle folding a case study from the Murtél rockglacier (Switzerland). *Permafrost Periglacial Process*. 2015;26(1):57-66. [PPP-14-0032.R2](https://doi.org/10.1016/j.geomorph.2018.03.015).
23. Anderson RS, Anderson LS, Armstrong WH, Rossi MW, Crump SE. Glaciation of alpine valleys: The glacier-debris-covered glacier - rock glacier continuum. *Geomorphology*. 2018;311:127-142. <https://doi.org/10.1016/j.geomorph.2018.03.015>
24. Arenson L, Springman S, Segó D. The rheology of frozen soils. *Appl Rheol*. 2007;17:12147-1.
25. Moore P. Deformation of debris-ice mixtures. *Rev Geophys*. 2014;52(3):435-467.
26. Haeberli W, Hoelzle M, Kaab A, Keller F, Vonder Muhl D, Wagner S. Ten years after drilling through the permafrost of the active rock glacier Murtél. In: Seventh International Conference on Permafrost; 1998; Yellowknife:403-410.
27. Haeberli W, Hunder J, Keusen H-R, Pika J, Rothlisberger H. Core drilling through rock-glacier permafrost. In: Fifth International Conference on Permafrost, Vol. 2; 1988; Trondheim:937-942.
28. Krainer K, Bressan D, Dietre B, et al. A 10,300-year-old permafrost core from the active rock glacier Lazaun, southern Ötztal Alps (South Tyrol, northern Italy). *Quaternary Res*. 2015;83:324-335.
29. Arenson L. pers. com; 2020.
30. Hanson S, Hoelzle M. The thermal regime of the active layer at the Murtél rock glacier based on data from 2002. *Permafrost Periglacial Process*. 2004;15:273-282.
31. Delaloye R, Lambiel C. Evidence of winter ascending air circulation throughout talus slopes and rock glaciers situated in the lower belt of alpine discontinuous permafrost (Swiss Alps). *Norsk Geografisk Tidsskrift - Norwegian J Geography*. 2005;59(2):194-203.
32. Scherler M, Schneider S, Hoelzle M, Hauck C. A two-sided approach to estimate heat transfer processes within the active layer of the Murtél-Corvatsch rock glacier. *Earth Surf Dyn*. 2014;2(1):141-154.
33. Wicky J, Hauck C. Numerical modelling of convective heat transport by air flow in permafrost talus slopes. *Cryosphere*. 2017;11(3):1311-1325.
34. Arenson L, Springman S. Mathematical descriptions for the behaviour of ice-rich frozen soils at temperatures close to 0 °C. *Canad Geotech J*. 2005;42(2):431-442.
35. Staub B, Marmy A, Hauck C, Hilbich C, Delaloye R. Ground temperature variations in a talus slope influenced by permafrost: a comparison of field observations and model simulations. *Geographica Helvetica*. 2015;70(1):45-62. <https://doi.org/10.5194/gh-70-45-2015>
36. Lugon R, Stoffel M. Rock-glacier dynamics and magnitude-frequency relations of debris flows in a high-elevation watershed Ritigraben, Swiss Alps. *Global Planet Change*. 2010;73(3):202-210.
37. Marcer M, Ringsø Nielsen S, Ribeyre C, et al. Investigating the slope failures at the Lou rock glacier front, French Alps. *Permafrost Periglacial Process*. 2020;31(1):15-30.
38. Kummert M, Delaloye R, Braillard L. Erosion and sediment transfer processes at the front of rapidly moving rock glaciers: Systematic observations with automatic cameras in the western Swiss Alps. *Permafrost and Periglacial Processes*. 2018;29(1):21-33.
39. Haeberli W, Vonder Muhl D. On the characteristics and possible origins of ice in rock glacier permafrost. *Zeitschrift für Geomorphologie, Supplementband*. 1996;104:43-57.
40. Haeberli W, Hallet B, Arenson L, et al. Permafrost creep and rock glacier dynamics. *Permafrost Periglacial Process*. 2006;17:189-214.
41. Hausmann H, Krainer K, Bruckl E, Ullrich C. Internal structure, ice content and dynamics of Ötztal and Kaiserberg rock glaciers (Ötztal Alps, Austria) determined from geophysical surveys. *Austr J Earth Sci*. 2012;105:12-31.
42. Clark D, Steig E, Potter NJ, Gillespie A. Genetic variability of rock glaciers. *Geografiska Annaler Ser A, Phys Geography*. 1998;80(3-4):175-182.
43. Humlum O. The geomorphic significance of rock glaciers: Estimates of rock glacier debris volumes and headwall recession rates in West Greenland. *Geomorphology*. 2000;35(1):41-67. [https://doi.org/10.1016/S0169-555X\(00\)00022-2](https://doi.org/10.1016/S0169-555X(00)00022-2)
44. Arenson L, Hauck C, Hilbich C, Seward L, Yamamoto Y, Springman S. Sub-surface heterogeneities in the Murtél-Corvatsch rock glacier, Switzerland. In: Proceedings of the Joint 63rd Canadian Geotechnical Conference and the 6th Canadian Permafrost Conference; 2010; Calgary, Canada:1494-1500.
45. Carslaw HS, Jaeger JC. *Conduction of heat in solids*, Oxford: Oxford University; 1959.
46. Krainer K, Mostler W. Hydrology of active rock glaciers examples from the Austrian Alps. *Arctic, Antarctic, Alpine Res*. 2002;34(2):142-149.
47. Bast A. pers. com; 2015.
48. Bucki A, Echelmeyer K. The flow of fireweed rock glacier, Alaska, U.S.A. *J Glaciology*. 2004;50(168):76-86.
49. Seppi R, Carturan L, Carton A, et al. Decoupled kinematics of two neighbouring permafrost creeping landforms in the eastern Italian Alps. *Earth Surface Process Landforms*. 2019;44:2703-2719.
50. Nye JF. The mechanics of glacier flow. *J Glaciology*. 1952;2(12):82-93.
51. Glen JW. The creep of polycrystalline ice. *Proc R Soc London A Math Phys Eng Sci*. 1955;228(1175):519-538.
52. Weertman J. Creep deformation of ice. *Ann Rev Earth Planet Sci*. 1983;11(1):215-240.

53. Mellor M, Testa R. Effect of temperature on the creep of ice. *J Glaciology*. 1969;8(52):131-145.
54. De La Chapelle S, Milsch H, Castelnaud O, Duval P. Compressive creep of ice containing a liquid intergranular phase rate-controlling processes in the dislocation creep regime. *Geophys Res Lett*. 1999;26(2): 251-254.
55. Cuffey K, Paterson WSB. *The physics of glaciers*. Burlington, MA: Butterworth-Heinemann/Elsevier; 2010.
56. Arenson L, Springman S. Triaxial constant stress and constant strain rate tests on ice-rich permafrost samples. *Canad Geotech J*. 2005;42 (2):412-430.
57. Ladanyi B. Rheology of icerock systems and interfaces. In: Proceedings of the eighth international conference on permafrost; 2003; Lisse, The Netherlands:621-625 (en).
58. Farinotti D, Brinkerhoff DJ, Clarke GKC, et al. How accurate are estimates of glacier ice thickness results from itmix, the ice thickness models intercomparison experiment. *Cryosphere*. 2017;11(2): 949-970.
59. Whalley WBrian, Martin HE. Rock glaciers ii models and mechanisms. *Progress Phys Geography Earth Environ*. 1992;16(2):127-186.
60. Groh T, Blothe J. Rock glacier kinematics in the kaunertal, otztal alps, Austria. *Geosciences*. 2019;9(9):373.
61. Czurda KA, Hohmann M. Freezing effect on shear strength of clayey soils. *Appl Clay Sci*. 1997;12(1):165-187.
62. Kellerer-Pirklbauer A, Lieb G, Kleinfirchner H. A new rock glacier inventory of the eastern european alps. *Austr J Earth Sci*. 2012;105 (2):78-93.
63. Jones DB, Harrison S, Anderson K, Betts RA. Mountain rock glaciers contain globally significant water stores. *Sci Rep*. 2018;8:2834-2844.
64. Marcer M, Serrano C, Brenning A, Bodin X, Goetz J, Schoeneich P. Evaluating the destabilization susceptibility of active rock glaciers in the french alps. *Cryosphere*. 2019;13(1):141-155.
65. PERMOS. Permafrost in Switzerland 2014/2015 to 2017/2018. In: Noetzli J, Pellet C, Staub B, eds. *Glaciological Report (Permafrost)No. 16-19 of the Cryospheric Commission of the Swiss Academy of Sciences*; 2019:104. <https://doi.org/10.13093/permos-rep-2019-16-19>
66. Marcer M, Bodin X, Brenning A, Schoeneich P, Charvet R, Gottardi F. Permafrost favorability index spatial modeling in the french alps using a rock glacier inventory. *Front Earth Sci*. 2017;5:105.
67. Delaloye R. pers. com; 2020.
68. Gruber S. Derivation and analysis of a high-resolution estimate of global permafrost zonation. *Cryosphere*. 2012;6(1):221-233. <https://www.the-cryosphere.net/62212012>
69. Dall'Asta E, Forlani G, Roncella R, Santise M, Diotri F, di Cella U. Unmanned aerial systems and dsm matching for rock glacier monitoring. *ISPRS J Photogrammet Remote Sens*. 2017;127:102-114.
70. Strozzi T, Caduff R, Jones N, et al. Monitoring rock glacier kinematics with satellite synthetic aperture radar. *Remote Sens*. 2020;12(3):559. <https://www.mdpi.com/2072-4292/12/3/559>
71. Kaab A, Vollmer M. Surface geometry, thickness changes and flow fields on creeping mountain permafrost automatic extraction by digital image analysis. *Permafrost Periglacial Process*. 2000;11(4):315-326.
72. Rohner C, Small D, Beutel J, Henke D, Luthi MP, Vieli A. Multisensor validation of tidewater glacier flow fields derived from synthetic aperture radar (sar) intensity tracking. *Cryosphere*. 2019;13(11): 2953-2975. <https://www.the-cryosphere.net/1329532019>
73. Lambiel C, Delaloye R, Strozzi T, Lugon R, Raetz H. Ers insar for assessing rock glacier activity. In: Proceedings of the 9th International Conference on Permafrost, Fairbanks, Alaska; 2008.
74. Barsch D. Permafrost creep and rockglaciers. *Permafrost Periglacial Process*. 1992;3(3):175-188.

SUPPORTING INFORMATION

Additional supporting information may be found online in the Supporting Information section at the end of this article.

How to cite this article: Cicoira A, Marcer M, Gärtner-Roer I, Bodin X, Arenson LU, Vieli A. A general theory of rock glacier creep based on in-situ and remote sensing observations. *Permafrost and Periglacial Process*. 2020;1-15. <https://doi.org/10.1002/ppp.2090>